Iranian Journal of Medical Physics

ijmp.mums.ac.ir

Investigating Motion Data Selections Based on Patient-Specific Respiration Pattern at External Surrogates Radiotherapy Using Cyberknife Synchrony Respiratory Tracking System

Seyed Amirreza Dastyar[1], Ahmad Esmaili Torshabi[1*]

1. Faculty of Sciences and Modern Technologies, Graduate University of Advanced Technology, Haftbagh Highway, Kerman, Iran

ARTICLE INFO

Article type:
Original Paper

Article history:
Received: Sep 09, 2023
Accepted: Feb 12, 2024

Keywords:
CyberKnife Radiosurgery
Tumor
Motion
Intelligent
Model

ABSTRACT

Introduction: : In order to personalize motion compensated radiotherapy with external surrogates, an intelligent method is proposed for selecting external surrogates' motion data on the basis of patient-specific respiration pattern. This strategy enhances targeting accuracy and can potentially feed the stereoscopic X-ray imaging system and lead to fewer imaging dose, intelligently.

Material and Methods: We investigate the effects of training data points firstly on correlation model construction at pre-treatment step for its training. Then, the same assessment will be done by means of updating data points on the model re-construction. Moreover, a recognition algorithm has been developed to detect high variability of breathing motion using pre-defined discriminator levels based on external motion amplitude.

Results: The number of training and updating data points can be intelligently optimized depending on the breathing pattern of each patient. In addition, by developing recognition algorithm, the shooting time for motion data selection is converted from conventional strategy to intelligent approach, accordingly. As example, for a patient with high motion variability while the number of critical data points recognized by our algorithm is significant, the targeting error with and without utilizing these data points are 4.4 mm and 6.6 mm, respectively.

Conclusion: This work promises to be aid a more personalized delivery of motion compensated radiotherapy using external surrogates by considering to motion data gathering, according to patient-specific respiration pattern. By implementing our strategy, we expect to make a compromise between the performance accuracy of correlation model and additional imaging dose.

►*Please cite this article as:*
Dastyar SA, Esmaili Torshabi A. Investigating Motion Data Selections Based on Patient-Specific Respiration Pattern at External Surrogates Radiotherapy Using Cyberknife Synchrony Respiratory Tracking System. Iran J Med Phys 2024; 21: 391-401. 10.22038/ijmp.2024.72269.2284.

Introduction

In Stereotactic Body Radiation Therapy (SBRT) due to high dose at single fraction, several efforts have been made to bring the delivered dose distribution closer to the planned one. [1]. But besides all those efforts, serious concerns on the accuracy of SBRT remain for dynamics tumors located in the chest and abdomen regions and move mainly due to respiration. One strategy is to combine the tumor volume and its likely position totally into an Internal Tumor Volume (ITV) as target for irradiating which lead to serious side effects [2].

Another solution is irradiation under breath hold to virtually immobilize the tumor, though this strategy requires upmost patient cooperation [3-5]. Alternatively, tumor motion gated radiotherapy [6-9] and real-time tumor tracking radiotherapy were introduced to compensate tumor motion error [10-13]. At two latter strategies, tumor position information must be extracted, by using additional motion monitoring systems, mounted in the treatment room [14].

A method for real-time tumor motion monitoring is the use of continuous X-ray imaging systems (i.e., fluoroscopy) [11, 15-16]. But, fluoroscopy as ionizing imaging modality violates the As Low As Reasonably Achievable (ALARA) concept [17]. To solve this problem, real-time tracking is most frequently strategy performed indirectly by means of external respiratory signals extracted from surrogates placed on the thorax region of the patient's body [13, 18]. The extracted signals are then inferred with the tumor motion using consistent correlation models. At our multiple previous studies, these correlation models have been demonstrated, comprehensively [19-28]. Furthermore, due to signal and system latencies, the external surrogate motion has to be predicted into the future (e.g., for 115ms for robotic radiosurgery) in order to allow the motion compensation to be in actual real-time [13, 18, 29]. This of course introduces

*Corresponding Author: Tel: +989386730223, Fax: +983426233166; Email: ahmad4958@gmail.com, a.esmaili@kgut.ac.ir

further errors and the quality of prediction modeling is also essential to the overall treatment accuracy [21, 29-31].

The overall performance accuracy of the correlation modeling system depends on two main parameters: 1) the model robustness and its statistical uncertainties, [25-27, 32-35] and 2) the numerical value along with acquisition time of the extracted external-internal motion dataset as highly important factor for defining the actual correlation model parameters and its performance, accordingly. In this work, we investigate the latter parameter in great detail by considering their effect on correlation model learning phase at pre-treatment step and also on model performance and its update on the basis of patient-specific respiration pattern that yield to better understanding of personalized radiotherapy.

For current clinical routine, the synchronized external internal motion data points are conventionally gathered within a routine and pre-defined period of time. Since, the breathing phenomena is highly variable for each patient, investigating the extracted data points and their acquisition time will be highly valuable in order to improve tumor motion tracking, while this issue has not been studied in great detail in the past. The proposed strategy in this study enhances targeting accuracy while it can potentially feed the stereoscopic X-ray imaging system and lead to fewer imaging dose, accordingly.

In order to reach this aim, the influence of training data points is evaluated on the parameters required during the building of the correlation model. This approach is then implemented on updating data points while the model will be re-constructed during the treatment. It worth mentioning that, the proposed algorithm is able to select the training and updating data points in an intelligent fashion on the basis of patient specific breathing behavior. To do this, a consistent recognition algorithm is developed to quantitatively realize the breathing motion behavior by means of pre-defined thresholds using the amplitude of external surrogates. This algorithm recognize patients with abnormal breathings and the correlation model will be further sensitized for tumor motion tracking by gathering sufficient training and updating data points, intelligently. It should be noted that we have implemented our strategy proposed in this work on our previously reported fuzzy logic-based correlation model [25-27] due to its robustness for the current investigation.

Final analyzed results illustrate that since each patient has its unique breathing pattern, the process of motion data acquisition can be changed from conventional fashion to intelligent mode. This is highly important for patient with abnormal breathing motion as our system demonstrated to be more sensitive and will take further images (model points) if needed over the course of the treatment. In contrast, for patients with regular breathing motion, our system will work with less data points and hence the patients imaging dose will be reduced, significantly. By this way, the most important data points are taken into account intelligently during patient respiration and the accuracy of correlation model construction and performance is increased remarkably that hence yield better treatment, compromising also with ALARA principle.

Materials and Methods

Patient database and motion properties

In this work, the external-internal motion datasets include synchronous data of the a) thorax surface motion and b) tumor position information from real patients treated with the Synchrony™ Respiratory Tracking System integrated with the CyberKnife™ robotic linear accelerator (Accuracy Incorporated, Sunnyvale, CA, USA) [13, 18]. The patients in this study were randomly selected from larger patient population with dynamic tumors in the thorax and abdomen regions. The external motion dataset was gathered by an infrared Optical Tracking System (OTS) responsible for monitoring (at 25 Hz update rate) three external Light Emitting Devices (LED) located on a vest that covers the rib cage and abdomen regions of the patient (Figure1).

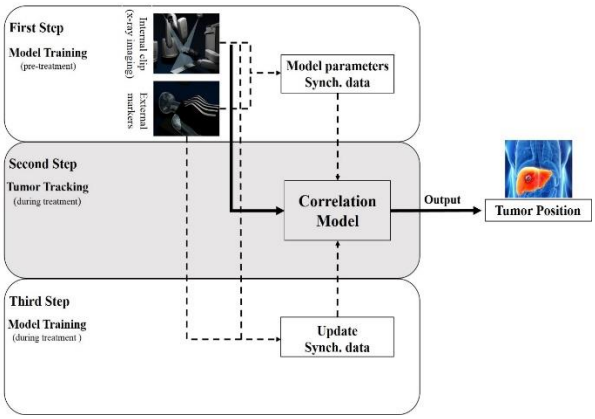

Figure 1. Block diagram of correlation model construction (first step), performance (second step) and update (third step)

The external dataset includes the (Three Dimensional) 3D position information of each of the three markers as a function of time which represents the continuous component of the respiratory signal. In contrast, the internal motion dataset represents the actual 3D tumor position information, i.e., in our case the location of implanted internal clip close to the tumor, and detected on stereoscopic X-ray images at various discrete time points over the respiratory cycle. Table 1 reports the 3D motion range of the tumor, external markers and treatment time.

Table 1. patient dataset including external markers and tumor motion properties (RLL: Right Lower Lung, LLL: Left Lower Lung, RUL: Right Upper Lung, SI: Superior-Inferior, AP: Anterior-Posterior, LR: Left-Right, STD: Standard Deviation)

	P1	P2	P3	P4	P5	P6	P7	P8	P9	P10
Tumor Location	RLL	LLL	PANCREAS	RIGHT HILUM	CHEST WALL	LEFT LUNG	RUL	LIVER	LEFT FLANK	LEFT SPLENIC BED
Tumor Motion on SI (mm)	31.1	70.5	15.8	18.2	2.6	55.8	4.0	18.7	3.0	2.0
Tumor Motion on LR (mm)	5.0	75.7	15.9	12.4	3.2	25.8	1.8	3.3	2.2	3.5
Tumor Motion on AP (mm)	3.8	31.9	12.0	7.7	7.7	40.7	6.4	7.8	2.4	4.3
External Motion (mm)	3.4	96.9	3.3	1.4	1.9	27	5.8	5.5	1.6	6.0
Imaging points Intervals (s), MEAN	66.9	41.0	55.8	73.7	63.6	71.9	97.6	64.5	58.1	81.7
Imaging points Intervals (s), STD	33.1	59.2	33.0	38.2	31.7	59.8	44.1	29.1	26.0	32.8
Total Treatment Time (min)	78.0	97.8	90.1	61.4	59.4	105.4	70.0	41.9	69.7	61.3

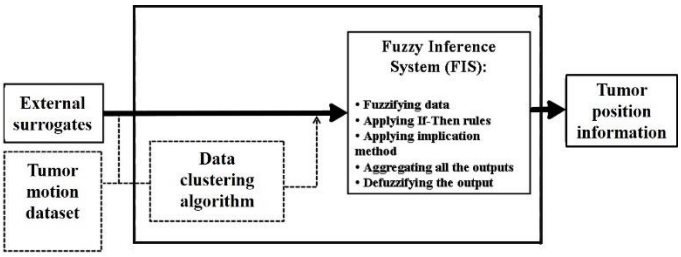

Figure 2. Fuzzy logic block diagrams

Correlation model and its configuration

According to our previous studies [26-27, 36-40], we utilized a correlation model based on fuzzy logic concept which appear to have a better accuracy in comparison to other common available modeling algorithms. We developed our model by using the MatLab software package (The MathWorks Inc., Natick, MA, USA) including the fuzzy logic toolbox which contains logical operations and *if-then* rules. As shown in figure 2, the correlation model is initially built using the training dataset during pre-treatment step (figure 1 first step).

Fuzzy Logic was introduced by Lotfi A. Zadeh [41-49] at 1965. Recently, fuzzy logic is recommended to give solutions for problems with qualitative, incomplete or imprecise information, while rigorous and analytical methods are not able to present precise solution. In fact, the fuzzy-based systems extend the classical two-valued modeling of concepts and attributes in a sense of gradual truth which can be used in the various fields and gives the better results regarding with conventional mathematical algorithms.

Membership functions at fuzzy logic systems are key components to realize demonstrate the magnitude of participation for each data point as input. At our proposed fuzzy correlation model data clustering (42-43) figure out the membership functions (Figure 2, lower dashed rectangle). After configuring, by given a data point as input, the Fuzzy Inference System works by a) data fuzzification, b) if-then rules induction, c) application of implication method, d) output aggregation and e) defuzzification steps (Figure 2).

In the correlation modeling system, the external markers position is denoted as $X(t)_{M1\text{-}M3}$, $Y(t)_{M1\text{-}M3}$ *and* $Z(t)_{M1\text{-}M3}$, where x, y and z are the 3D coordinates of markers (M_1 - M_3) at time *t*. The internal tumor position (i.e., in our case the internal clip) is denoted as $X(t)_C$, $Y(t)_C$ and $Z(t)_C$, where x, y and z are the 3D coordinates of the clip (C) at time *t*. The position dataset is then represented in a matrix where each row represents synchronous paired data points of external markers and internal clip at time point t_n (Figure 3).

First of all, the model is constructed with a certain number of data points recorded at various time points in the respiratory cycles during the training phase (patient alignment). Once the model is visually to the users' satisfaction, the system is ready for treatment (figure 1, second step). Note that currently there is no real qualitative feedback for the overall model accuracy. Only the last point fit accuracy is determined by providing a so called correlation error. Furthermore, the completeness over the full and mostly irregular breathing cycle is also not determined, but only the point coverage over the last few minutes is provided.

During treatment, the model performance accuracy is tested by routinely and the model can also be updated periodically (figure 1, third step). For this purpose, stereoscopic X-ray images are taken at several intermittent time points (e.g., every minute, conventionally [28, 30]), as illustrated in figure 4. The model accuracy at each time point during the treatment

should be in an acceptable positional uncertainty range, otherwise the tumor motion tracking is not accurate and the model must be rebuilt, completely [30]. It should be noted that the total treatment time varies from 42 to 90 minutes in our patients' group.

Optimization of synchronous motion dataset extraction

Model performance and update phase: Assuming correlation model construction, it's ready to infer tumor trajectory using only external markers dataset, as input. If model was trained as well with proper breathing pattern, critical motions are not known for modeler, and otherwise its performance may yield to large targeting errors.

In this phase we consider to specific times of treatment process, while new recorded data points (taken by motion monitoring systems) are utilized for model testing and updating. This ensure us to realize that the targeting error of our model is in acceptable uncertainty range. Furthermore, the model can be rebuilt using new arrival paired data points.

In this study, firstly the numbers of updating steps and also the time intervals between those updates are investigated for each patient.Moreover, the role or the importance degree of each update step is taken into account, quantitatively by removing some update data points throughout treatment process and calculating model performance accuracy.

For this assessment, different patients with normal and abnormal breathing motion are considered by measuring the amplitude of external markers motion. At cases with abnormal respiration, the behavior of external markers is highly variable with large amplitudes out of normal range and we interestingly focus on these cases to investigate our proposed strategy.

It's worth mentioning that, our findings at performing and updating phases reach us to a compromise between model accuracy and ALARA principle. Our results will define a new framework at SBRT to reduce additional imaging dose while keeping treatment quality in acceptable level at same time.

In this work, motion dataset of tumor and thorax surface is taken into account at two phases in order to avoid ambiguity: a) at pre-treatment step, while the model is learning by means of training data points and b) during treatment, while the model is tracing tumor motion using only thorax surface motion signal. At latter phase, the model performance is also tested and its structure is re-configured for better tracing with less uncertainty error.

Model learning phase: The success degree of each learning based correlative model, depends highly on the properties of training dataset. In our case, training data points must represent a good pattern of respiration and tumor motion by covering all possible variabilities of motion amplitudes and frequencies. To do this, the number of training data points and their acquisition time are highly important to lead a proper correlation model construction. It should be noted that the number of training data points is not essentially constant for each patient and even for each fraction of a given patient during total treatment course.

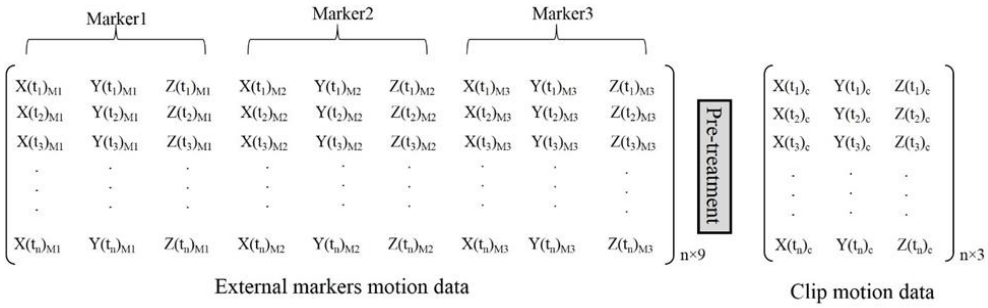

Figure. 3 matrices of 3D position information of three external markers with *n×9* size (left side) and 3D position information of implanted internal clip representing tumor with *n×3* size (right side) at pre-treatment step, *n* is # of paired data points

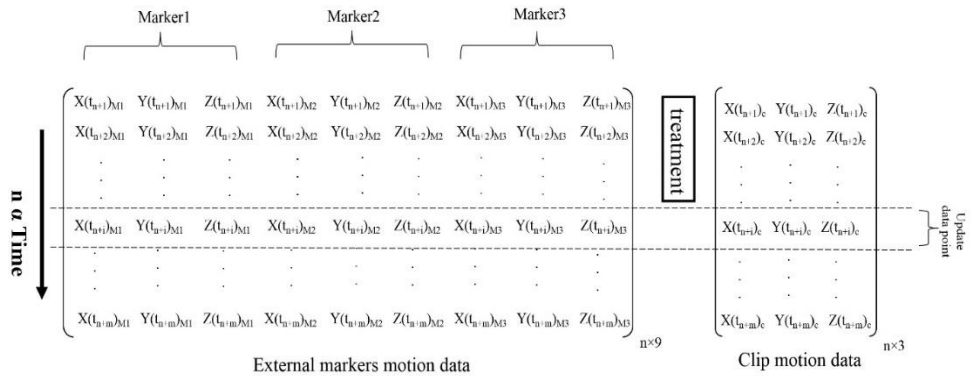

Figure 4. matrices of 3D position information of three external markers with *n×9* size (left side) and 3D position information of implanted internal clip representing tumor with *n×3* size (right side) at pre-treatment step

First of all, the effect of the number of training dataset on model construction at learning phase is considered. Our patient's dataset is as time series log files in ASCII format and the number training data points of each patient are easily accessible to be changed in time stamp file. In fact, each recorded data point has its membership activation code and therefore a training data point at pre-treatment can belong to update point at treatment by manipulating its membership activation code and vice versa. Using this strategy, various models are configured with various Number of Training Data points (NTD) for each patient and targeting errors of the models can be compared with each other and also with CK modeler, applied clinically.

Determination of abnormalities in breathing phenomena during treatment

Furthermore, we developed an additional subroutine to sensitize the monitoring systems against abnormal motion changes or strange amplitude with adjustable sensitivity degree. Specifically, through the degree of motion variation of the external markers during treatment, each time point can be classified as potentially critical or noncritical to the correlation model. To classify the degree of motion variation, the amplitude of the external markers motion is compared with the average value calculated from a group of recorded external markers motion amplitudes as required component for model building and updating. This average value is calculated according to the following formula:

$$A_{ave} = 2/NTD \sum_{n=1}^{n=NTD/2} (A_{ext}(n)) \quad (1)$$

Where *NTD* is the number of training data points, A_{ext} is the amplitude of each external marker motion.
If the current amplitude of the external marker motion is classified as critical for the current correlation model, the subroutine would trigger a new data point acquisition from the stereoscopic X-ray imager in order to update the model. Otherwise, if the current amplitude is classified as noncritical, the system would delay further imaging in order to reduce imaging dose to the patient. By implementing this strategy, stereoscopic X-ray imager act intelligently to feed the correlation model regarding with conventional clinical methods. Moreover, this strategy leads imaging dose reduction for patients with normal breathing.

Results

The NTD of our patient group ranged from 6 to 15. It should be noted that our patients were randomly selected with no considering to tumor type or site. We investigated the role of each synchronous paired data point as a) trainer during model learning phase and b) as tester and updater during model performance phase.

Figure 5 shows the variation of NTD on Root Mean Square Error (RMSE) over 10 patients. As example in lower left sub-plot, with our fuzzy logic method we determined an optimum NTD with 6 data points that yielded the least RMSE. This NTD is less than the NTD needed for the currently utilized clinical correlation model (8 data points). Such NTD reduction would have saved the patient from at least two shots of stereoscopic X-ray imager during the model learning phase alone and without any reduction in correlation modeling accuracy.

It should be noted that the parameters of correlation model are same for each NTD at each case in order to obtain the effect of NTD variation on 3D targeting error. As resulted from this figure, there is an optimum NTD for each patient, accordingly. As seen, at some cases the differences among clinical and optimal NTD are remarkable. Since each patient has its unique breathing pattern, we cannot implement the same strategy of obtaining a constant number for training data points. On one hand, the NTD value should be high enough to cover the full parts of the regular and irregular breathing cycles. On the other hand, by raising the NTD the total imaging dose received by patient will be increased which must be considered according to ALARA principle. Moreover, less NTD will result in less performance accuracy of the correlation model for tumor tracking.

Figure 6 shows the 3D position information of synchronized external markers and the tumor motion coordinates during initial correlation modeling for a typical patient. The training dataset for this patient includes nine data points which for our fuzzy logic method are clustered and then membership functions with if-then rules are applied for model parameter definition. The irregular spatial distribution of training data points that results variable clustering, has been shown in this figure.

As mentioned before, another effect of each training data point is its acquisition time. The data points must be well distributed over the breathing cycles as a function of time. Figure 7 illustrates the importance degree of data points taken from marker 1 of a given patient with right lower lung cancer. We assessed the peaks and valleys of each marker motion as critical point versus time. For example, at sub-plots depicting the position of external marker #1, the second data point is in the valley position for the X (LR) direction while this point is in the peak position for the Y (AP) and Z (SI) directions. Hence, we considered this data point as critical for correlation modeling.

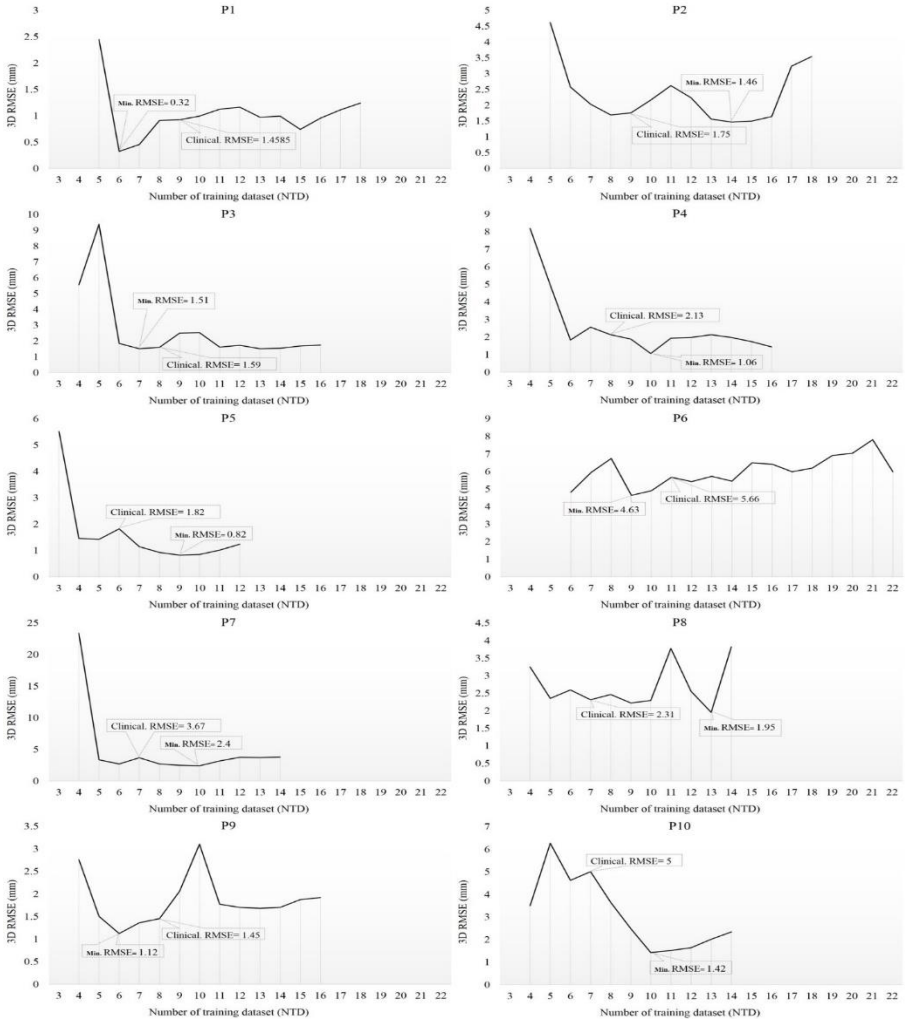

Figure 5. The effect of different NTD on the targeting error of the correlation model

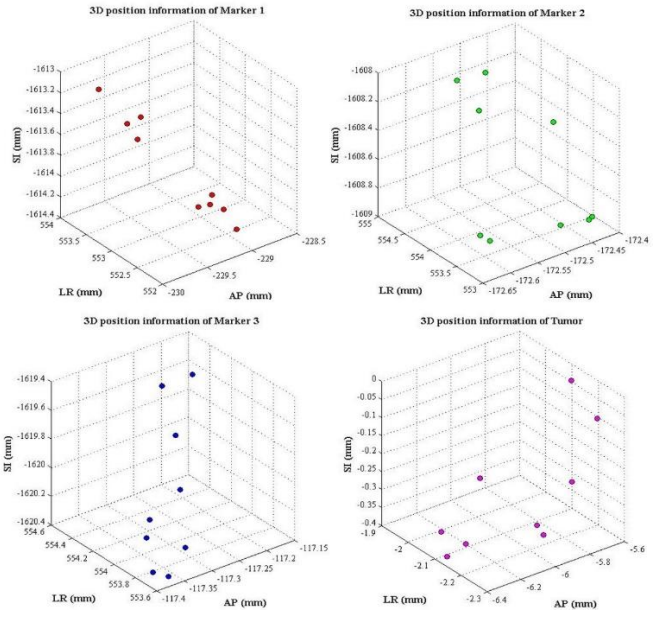

Figure 6. 3D spatial coordinate of external marker 1(upper right) external marker 2(upper left) external marker 3(lower right) and tumor position (lower left) representing training dataset gathered at pre- treatment step

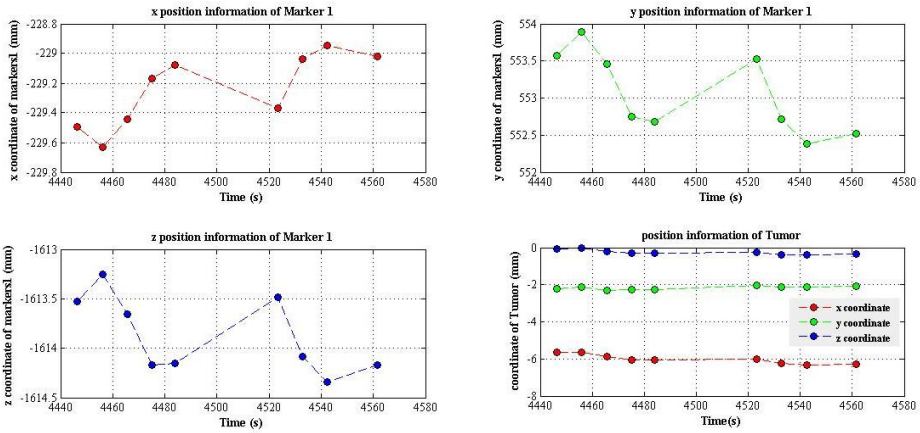

Figure 7. position information of external marker 1 at x (upper left) y (upper right) and z (lower left) directions representing importance degree of data point and tumor position (lower right) as function of time at pre-treatment step

Table 2. RMSE calculated with and without selected training data points

patient No.	data point index (removed)	RMSE of model using all training data points (mm)	RMSE of model without removed data points (mm)	Error increasing percentage of column 4 vs. column 3 (%)
P1	8	0.93	1.04	11
	2	0.93	1.037	11.83
P2	2	1.76	3.22	83.72
	9	1.76	3.41	94.34
P3	6	1.59	10.06	529.43
	3	1.59	9.99	524.74
P4	7	2.14	2.58	20.00
	2	2.14	2.49	16.42
P5	5	1.82	2.18	19.58
	2	1.82	2.16	18.35
P6	11	5.66	8.47	49.73
	3	5.66	8.87	56.71
P7	4	3.67	11.69	318.52
	3	3.67	5.37	46.42
P8	2	2.313	3.04	31.45
	4	2.31	3.00	29.78
P9	1	1.46	2.91	99.36
	6	1.46	1.58	8.35
P10	2	5.01	5.504	9.88
	6	5.01	5.70	13.81

Table 2 shows the importance degree of some training data points. For this aim, some data points belonging to specific parts of respiratory cycle and classified as critical data points (such as peak or valley points) have been removed and the correlation model was constructed with and without those data points. In fact, each data point has its unique value (weight) in the correlation model. For some data points their weights are very similar and hence their degree of importance is almost the same. To be explicit, for constructing a robust correlation model enough data points covering all motion variations which are also well distributed over the breathing cycles are required in order to allow the best model learning process.

After investigating the effect of each NTD for the pre-treatment setup, we assessed the same strategy for update data points during the treatment. For this aim, we developed a subroutine which acts as discriminator for detecting critical data points. The basis of our discriminator operation is comparing the amplitude of external motion data with the average value of prior motion data points. It should be noted that the sensitivity degree of this subroutine is adjustable and can be numerically controlled. Figure 8 shows a critical data point belonging to motion information of one external marker for a given patient with left lower lung cancer. As seen, this data point has been extracted by means of our mathematical statistical subroutine as discriminator.

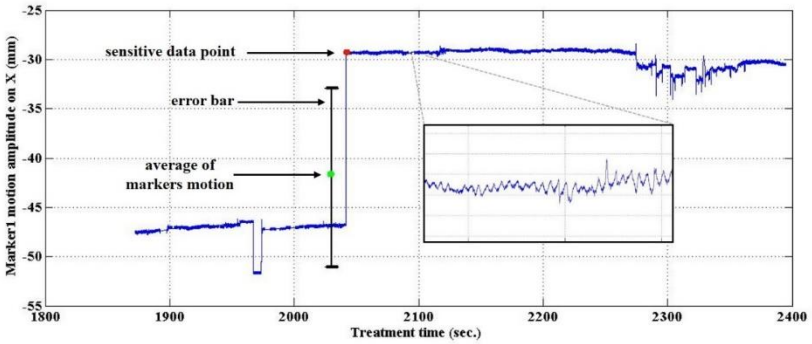

Figure 8. motion amplitude of marker #1 over total treatment time representing the performance of mathematical statistical subroutine for extracting critical data points (red point), green point is the average of markers motion in a pre-defined time shown with error bar

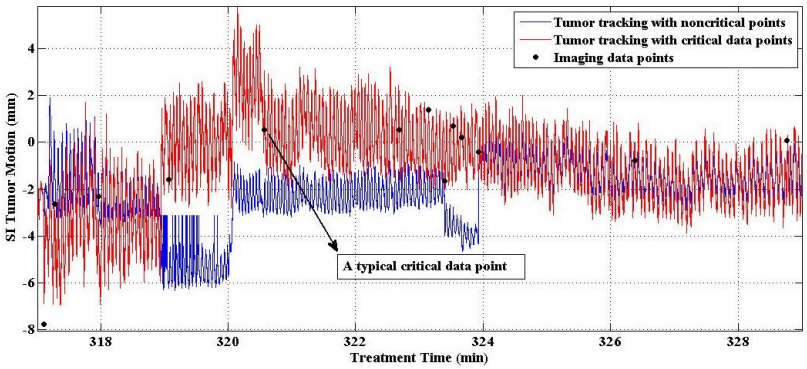

Figure 9. Tumor tracking for a given patient on SI direction at specific treatment time interval with noncritical imaging data points (blue) and with critical data points (red)

Figure 9 represents the important role of critical data points among the dataset required for model reconstruction during the treatment. This figure includes a comparative depiction between two conditions with a) noncritical data points (blue line) and b critical data points (red line). The critical data points shown in this figure are located at the middle part of total treatment time. As illustrated in this figure, tumor tracking is more precise in presence of critical data points.

Discussion

In current clinical practice, stereotactic body radiotherapy is increasingly performed using external surrogates while fluoroscopy-based tracking is rarely used in order to minimize additional imaging dose. In ideal form, tumor motion monitoring must be done with highest possible targeting accuracy while using the least X-ray imaging data points in order to fulfill the ALARA principle. In external surrogate radiotherapy, stereoscopic X-ray imaging as tumor monitoring system provides data points intermittently for correlation model construction before treatment and also for its performance testing and updating during the treatment.

In this treatment modality, the first problem that must be addressed refers to performance accuracy of correlation model, which significantly depends on two main facts. Firstly, the type and inherent mathematical structure of utilized model that is the basis for an accurately dose delivery. We previously investigated targeting accuracy of several available linear and non-linear correlation models as comparative studies while implementing various mathematical methods with variable model parameters definition and demonstrated the superiority of fuzzy logic-based model regarding with the other modelers [26, 27, 32-34]. Secondly, the properties of external-internal motion dataset gathered at before and during treatment that significantly impact on the model algorithm performance. Both factors are highly variable as our main objective in the presented study to comprehensively investigate the motion dataset properties and the procedure of data gathering without any concern to correlation model type and underlying mathematical structure.

For this aim, the acquisition time of monitoring systems are important and data points with high degree of importance for the correlation model must be gathered. Based on our database analysis, , we found that the captured data points must not be spatially concentrated only around a specific part of breathing cycle, but they must be well distributed over the whole breathing cycles during the pre-treatment model learning phase. By this strategy, the numerical values of data points will be significantly different to each other and in the wide range of motion amplitude.

The first challenging issue for us in this work was investigation of the role of synchronous data points recorded during patient setup. Apparently, the optimized training dataset at both quantity and their acquisition time will yield a well-trained model with lowest tracking error and lowest imaging dose to the patient.

Without these optimal factors either the model may not fit the actual target motion as well and hence result in target miss or the imaging dose will be very high when multiple redundant model points are taken. It should be noted that, the same concept is true during the treatment as second challenge we implemented the same strategy to evaluate how often model updating is required and when the best time for a model update is indicated.

According to the results shown in figure 4, the number of training data points taken by Cyberknife synchrony system are far from being optimal at some cases. By changing NTD, the calculated errors were reduced using our proposed method in comparison to the utilized NTD in real clinical condition. As resulted from our study, the NTD collected at model learning phase must be large enough to represent a reasonable pattern of real breathing cycles of the patient. The findings shown at figure 5 illustrates that the NTD values can be determined in an intelligent manner. Since higher NTD may cause receiving additional imaging dose to the patient and lower NTD may result weak correlation model, an optimum value is highly advised in this section.

Moreover, in order to assess the importance degree of each data point at pre-treatment step, we investigated this issue by removing it from the model dataset during training and calculating the according model output. The model output and the calculated targeting error with and without a given data point allowed the determination if the point is critical or noncritical to the model performance. In fact, when removing important points from the model, such as valley or peak point in the breathing cycle (figure 7), the targeting error remarkably increases pointing to a high importance degree of those data points.

Finally, we added a subroutine to the correlation model to significantly increase the sensitivity of the monitoring systems according to breathing motion variations. A good strategy appears to be, that both internal and external motion monitoring systems will capture data points while breathing motion amplitudes are out of their normal range and even more so during respiration baseline changes which may happen frequently [28]. The detection of such these abnormalities however is no small task and for our method it was based on a mathematical subroutine added to our developed algorithm. This subroutine works by using the past amplitude of breathing cycles and is able to extract abnormal breathings on the fly. Figure 6 showed the implemented mathematical method for critical data point extracting and figure 7 illustrated the importance degree of such these data points on tumor tracking accuracy.

The proposed strategy can be very effective for patients with abnormal breathing variations and should be considered for general clinical routine. Constructing a proper model with as minimal data points as possible is important and we expect to make better judgment for trade-off between the performance accuracy of correlation model and additional imaging dose delivered by stereoscopic X-ray system.

It's worth mentioning that the current effort promises to be aid a more personalized delivery of motion compensated radiotherapy using external surrogates. Future study will focus on data clustering and intelligent stereoscopic X-ray imager based on a large patient group considering motion behavior of each dynamic tumor, in a comparative fashion.

Conclusion

In this work, we investigated the properties of pre-treatment and in-treatment motion datasets required for correlation model construction and updating during radiotherapy with external surrogates. For correlation modeling at both learning and performance phases we found two dominating factors: a) the number of data points must be sufficient and b) the importance degree of each data point must be significant. The latter factor refers directly to data point acquisition time. Various condition for correlation modeling were assessed and uncertainty errors of the correlation model was considered to represent the best targeting accuracy. We found that breathing motions variability must be intelligently taken into account during training and updating the correlation model in order to ensure a high-quality radiotherapy treatment.

Acknowledgment

The authors acknowledge Sonja Dieterich (Sacramento, CA, USA) for providing access to the clinical database.

References

1. Tomas K. Reduction of margins in external beam radiotherapy. Journal of Medical Physics. 2008;33(2):41–2.
2. Shih HA, Jiang SB, Aljarrah KM, Doppke KP, Choi NC. Internal target volume determined with expansion margins beyond composite gross tumor volume in three-dimensional conformal radiotherapy for lung cancer. International Journal of Radiation Oncology Biology Physics. 2004;60(2):613-22.
3. Hanley J, Debois MM, Mah D, Mageras GS, Raben A, Rosenzweig K, et al. Deep inspiration breath-hold technique for lung tumors: the potential value of target immobilization and reduced lung density in dose escalation. International Journal of Radiation Oncology* Biology* Physics. 1999 Oct 1;45(3):603-11.
4. Mah D, Hanley J, Rosenzweig KE, Yorke E, Braban L, Ling CC, et al. Technical aspects of the deep inspiration breath-hold technique in the treatment of thoracic cancer. International Journal of Radiation Oncology* Biology* Physics. 2000 Nov 1;48(4):1175-85.
5. Rosenzweig KE, Hanley J, Mah D, Mageras G, Hunt M, Toner S, et al. The deep inspiration breath-hold technique in the treatment of inoperable non–small-cell lung cancer. International Journal of Radiation Oncology* Biology* Physics. 2000 Aug 1;48(1):81-7.

6. Minohara S, Kanai T, Endo M, Noda K, Kanazawa M. Respiratory gated irradiation system for heavy-ion radiotherapy. International Journal of Radiation Oncology Biology Physics. 2000;47:1097-03.
7. Kubo HD, Hill BC. Respiration gated radiotherapy treatment: A technical study. Physics in Medicine and Biology. 1996;41:83-91.
8. Ohara K, Okumura T, Akisada M, Inada T, Mori T, Yokota H, et al. Irradiation synchronized with respiration gate. International Journal of Radiation Oncology* Biology* Physics. 1989 Oct 1;17(4):853-7.
9. Shirato H, Shimizu S, Kunieda T, Kitamura K, Van Herk M, Kagei K, et al. Physical aspects of a real-time tumor-tracking system for gated radiotherapy. International Journal of Radiation Oncology* Biology* Physics. 2000 Nov 1;48(4):1187-95.
10. Booth JT, Caillet V, Hardcastle N, O′Brien R, Szymura K, Crasta C, et al. The first patient treatment of electromagnetic-guided real time adaptive radiotherapy using MLC tracking for lung SABR. Radiotherapy and Oncology. 2016 Oct 1;121(1):19-25.
11. Shirato H, Shimizu S, Shimizu T, Nishioka T, Miyasaka K. Real-time tumor-tracking radiotherapy. Lancet. 1999;353:1331-2.
12. Kamino Y, Takayama K, Kokubo M, et al. Development of a four-dimensional image-guided radiotherapy system with a gimbaled X-ray head. International Journal of Radiation Oncology Biology Physics. 2006;66(1):271-8.
13. Schweikard A, Glosser G, Bodduluri M, Murphy MJ, Adler JR. Robotic motion compensation for respiratory movement during radiosurgery. Computed Aided Surgery. 2000;5:263–77.
14. Dawson LA, Sharpe MB. Image-guided radiotherapy: rationale, benefits, and limitations. Lancet Oncology. 2006;7:848–58.
15. Xu Q, Hamilton RJ, Schowengerdt RA, Alexander B, Jiang SB. Lung tumor tracking in fluoroscopic video based on optical flow. Medical Physics. 2008;35:5351–9.
16. Lin T, Cervino LI, Tang X, Vasconcelos N, Jiang SB. Fluoroscopic tumor tracking for image-guided lung cancer radiotherapy. Physics in Medicine and Biology. 2009;54:981–92.
17. Keall PJ, Mageras GS, Balter JM. The Management of Respiratory Motion in Radiation Oncology report of AAPM task group 76. Medical Physics. 2006;33:3874-900.
18. Kilby W, Dooley JR, Kuduvalli G, Sayeh S, Maurer Jr CR. The CyberKnife Robotic Radiosurgery System in 2010. Technology in Cancer Research and Treatment. 2010;9(5):433-52.
19. Seppenwoolde Y, Berbeco RI, Nishioka S, Shirato H, Heijmen B. Accuracy of tumor motion compensation algorithm from a robotic respiratory tracking system: a simulation study. Medical Physics. 2007;34:2774-84.
20. Hoogeman M, Prevost JB, Nuyttens J, Pöll J, Levendag P, Heijmen B. Clinical accuracy of the respiratory tumor tracking system of the cyberknife: assessment by analysis of log files. Radiation Oncology. 2009;74:297-303.
21. Pepin EW, Wu H, Zhang Y, Lord B. Correlation and prediction uncertainties in the cyberknife synchrony respiratory tracking system. Medical Physics. 2011;38(7):4036-44.
22. Ernst F, Bruder R, Schlaefer A, Schweikard A. Correlation between external and internal respiratory motion: a validation study. International Journal of Computer Assisted Radiology and Surgery. 2012;7(3):483-92.
23. Poels K, Dhont J, Verellen D. A comparison of two clinical correlation models used for real-time tumor tracking of semi-periodic motion: A focus on geometrical accuracy in lung and liver cancer patients. Radiotherapy and Oncology. 2015;115(3):419-24.
24. Yan H, Yin FF, Zhu GP, Ajlouni M, Kim JH. The correlation evaluation of a tumor tracking system using multiple external markers. Medical Physics. 2006;33:4073–84.
25. Torshabi AE, Pella A, Riboldi M, Baroni G. Targeting accuracy in real-time tumor tracking via external surrogates: a comparative study. Technology in Cancer Research and Treatment. 2010;9:551–62.
26. Torshabi AE, Riboldi M, Imani Fooladi AA, Modarres Mosalla SM, baroni G. An adaptive fuzzy prediction model for real time tumor tracking in radiotherapy via external surrogates. Journal of Applied Clinical Medical Physics. 2013;14:102-14.
27. Torshabi AE. Investigation the Robustness of Adaptive Neuro-Fuzzy Inference System for Tracking of Moving Tumors in External Radiotherapy. Australasian Physical and Engineering Sciences in Medicine. 2014;37:771-8.
28. Malinowski K, McAvoy TJ, George R. Incidence of changes in respiration-induced tumor motion and its relationship with respiratory surrogates during individual treatment fractions. International Journal of Radiation Oncology Biology Physics. 2012;82(5):1665-73.
29. Ernst F, Schlaefer A, Schweikard A. Predicting the outcome of respiratory motion prediction. Medical Physics. 2011;38(10):5569-81.
30. Malinowski KT, McAvoy TJ, George R, Dietrich S, D'Souza WD. Mitigating errors in external respiratory surrogate-based models of tumor position. International Journal of Radiation Oncology Biology Physics. 2012;82(5):709-716.
31. Ernst F, Dürichen R, Schlaefer A, Schweikard A. Evaluating and comparing algorithms for respiratory motion prediction. Physics in Medical and Biology. 2013;58(11):3911-3929.
32. Kakar M, Nyström H, Aarup LR, Nøttrup TJ, Olsen DR. Respiratory motion prediction by using the adaptive neuro fuzzy inference system (ANFIS). Physics in Medicine and Biology. 2005;50:4721-8.
33. Riaz N, Shanker P, Gudmundsson O. et al. Predicting respiratory tumor motion with Multi-dimensional Adaptive Filters and Support Vector Regression. Physics in Medicine and Biology. 2009;54:5735-18.
34. Vedam SS, Keall PJ, Docef A. Todor DA, Kini VR, Mohan R. Predicting respiratory motion for four-dimensional radiotherapy. Medical Physics. 2004;31:2274–83.

35. Ruan D, Fessler JA, Balter JM, Berbeco RI, Nishioka S, Shirato H. Inference of hysteretic respiratory tumor motion from external surrogates: a state augmentation approach. Physics in Medicine and Biology. 2008;53:2923-36.
36. Ghorbanzadeh L, Torshabi AE, Soltani Nabipour J, Ahmadi Arbatan M. Development of a Synthetic Adaptive Neuro-fuzzy Prediction Model for Tumor Motion Tracking in External Radiotherapy by Evaluating Various Data Clustering Algorithms. Technology in Cancer Research and Treatment. 2016;15(2):334-7.
37. Torshabi AE, Ghorbanzadeh L A study on stereoscopic X-ray imaging data set on the accuracy of real time tumor tracking in external bean radiotherapy. Technology in Cancer Research and Treatment. 2017;16(2):167–77.
38. Nankali S, Torshabi AE, Samadi Miandoab P. A feasibility study on ribs as anatomical landmarks for motion tracking of lung and liver tumors at external beam radiotherapy. Technology in Cancer Research and Treatment. 2017;16(1):99–111.
39. Samadi Miandoab P, Torshabi AE, Nankali S. investigation of optimum location of external markers for patient setup accuracy enhancement at external beam radiotherapy. Journal of Applied Clinical Medical Physics. 2016;17(6):32–42.
40. Samadi Miandoab P, Torshabi AE, Parandeh S. calculation of inter-and intra-fraction motion errors at external radiotherapy using a markerless strategy based on image registration combined with correlation model. Iranian Journal of medical physics. 2019;6(3):224-31.
41. Zadeh LA. Fuzzy Sets. Information and Control. 1965;8:338-53.
42. Zadeh LA. Outline of a New Approach to the Analysis of Complex Systems and Decision Processes. IEEE Transactions on Systems, Man, and Cybernetics. 1973;3:28-44.
43. Zadeh LA. Fuzzy algorithms. Information and Control. 1968;12:94-102.
44. Zadeh LA. Fuzzy Logic. Computer. 1988;1:83-93.
45. Zadeh LA. Knowledge representation in fuzzy logic. IEEE Transactions on Knowledge and Data Engineering. 1989;1:89-100.
46. Jain AK, Murty MN, Flynn PJ. Data clustering: a review. ACM Computing Surveys. 1999;31:264-323.
47. Jang J, Chuen-Tsai S, Mizutani E. Neuro fuzzy modeling and soft computing. Englewood Cliffs, Prentice-Hall; 1997.
48. Jang J. ANFIS: adaptive-network-based fuzzy inference system. IEEE Transactions on Systems, Man, and Cybernetics. 1993;23:665–85.
49. Chiu S. Fuzzy Model Identification Based on Cluster Estimation. Journal of Intelligent & Fuzzy Systems. 1994;2:267-78.